

### 2.1 Experimental details:

Chapter 2 provides a detailed description of the procedures and techniques used for synthesizing the materials and characterizing their physical properties.

This part starts with the methodological demonstrations and steps used in the preparation of various compounds which have been used in our whole research works and this part is then followed by different experimental techniques used for investigating the various properties of the desired systems.

#### 2.1.1 Sample synthesis technique: Solid state reaction method

The conventional solid state reaction method for oxide polycrystalline solid sample synthesis is one of the most widely used techniques which use a stoichiometric mixture of different starting powder materials as precursors. At room temperature, solids do not react with each other over normal time scales and thus, it is required to heat them to quite high temperatures, often to 1000 to 1500 °C so that the reactions may take place at an appreciable rate. The key factors which mainly decide the feasibility and rate of a solid state reaction are the reaction conditions, surface area of the solids, structural properties of the reactants, and their reactivity and the thermodynamic free energy change related to the reaction.

In throughout our research work, the highly pure oxide powder materials have been used. The powders were taken in proper stoichiometry and then it was intimately ground for 1-2 hours in an agate mortar. This thoroughly mixed powder was then subjected to an initial heat treatment at a desired temperature (900-1000<sup>0</sup> C). Once the temperature reaches the room temperature, the powder was reground and then it was put in a muffle furnace in air at different desired temperatures (up to 1200<sup>0</sup> C) for several days followed by intermittent grindings to get the pure phase formation. This was then ground finely and it was used to

carry out the powder X-ray diffraction experiment at room temperature to check the phase purity. Finally, this powder was pressed into pellets using the hydraulic press under suitable pressure for final sintering at some higher temperatures depending on the systems (1250-1400<sup>0</sup> C). These sintered samples were undergone through different experiments to explore their properties, for example, structural, magnetic, spectroscopic, optical, electrical etc. The detailed processes have been discussed in the working chapters. The generalized flow chart for the solid state reaction techniques is show in below:

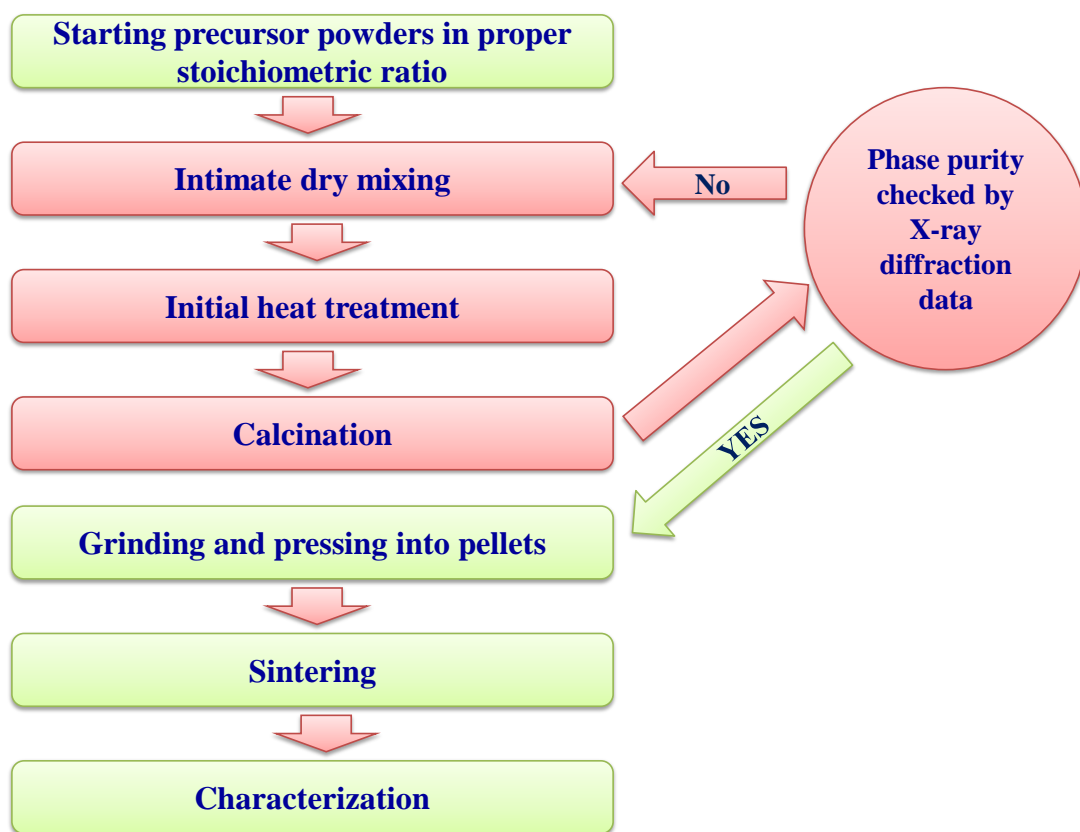


**Figure. 2.1:** *The general flow chart for solid state reaction method.*

### 2.1.2 Characterizing instruments and their brief working principle

#### 2.1.2.1 X-ray diffractometer:

The X-ray powder diffraction (XRD) technique is a rapid analytical and non-destructive technique which is primarily used for phase identification of a crystalline material and is also capable of providing information of unit cell dimensions. The material used for this experiment requires finely ground, homogenized powder and average bulk composition is obtained.

##### 2.1.2.1.1 Basic principles of X-ray powder diffraction (XRD) method:

In the year of 1912, Max von Laue first discovered that crystalline materials act as three-dimensional diffraction gratings for X-ray wavelengths similar to the spacing of planes in a crystal lattice. Hence, XRD has now become a common technique for the investigations of crystal structures and crystalline size etc. The X-ray diffraction is based on constructive interference of monochromatic X-rays in a crystalline lattice. The X-ray beams are produced by a cathode ray tube which is then filtered to get monochromatic radiation, collimated to concentrate, and finally directed toward the sample under investigation. The interaction of the incident X-rays with the sample results in the constructive interference producing a diffracted ray when conditions of Bragg's Law ( $2d \sin \theta = n\lambda$ ) gets satisfied. This law correlates the wavelength of electromagnetic radiation to the diffraction angle and the lattice spacing in a crystalline sample. These diffracted X-rays are then detected, processed and counted. The all possible diffraction directions of the lattice is covered by scanning the sample through a wide range of  $2\theta$  angles (because of the random orientation of the powdered material). Eventually, the conversions of the diffraction peaks to the corresponding d-spacings allow one to identify

a particular crystalline compound because each such compound has a unique set of d-spacings. Generally, this is done by comparing the d-spacings with standard reference data.

### 2.1.2.1.2 The experimental setup used:

In performing the XRD experiments, a monochromatic X-ray radiation of copper source ( $\text{Cu-K}\alpha = 1.5418\text{\AA}$ ) have been used. A collimated beam of X-ray strikes the sample kept in powdered form on a glass slab and it produces the diffracted beams. This beam is collected by employing a moveable detector such as a Geiger counter, a scintillation counter or image plate which is linked to the chart recorder. X-ray diffraction set-up has been demonstrated in Fig. 2.2. In regular use, the counter is driven to scan at a constant angular velocity over an angular range of  $2\theta$  values (typically, we have used 10 to 90 degree). In fact, the identification of single or multiple phases of a system allows us to get an idea of the mechanism behind the formation of the sample.

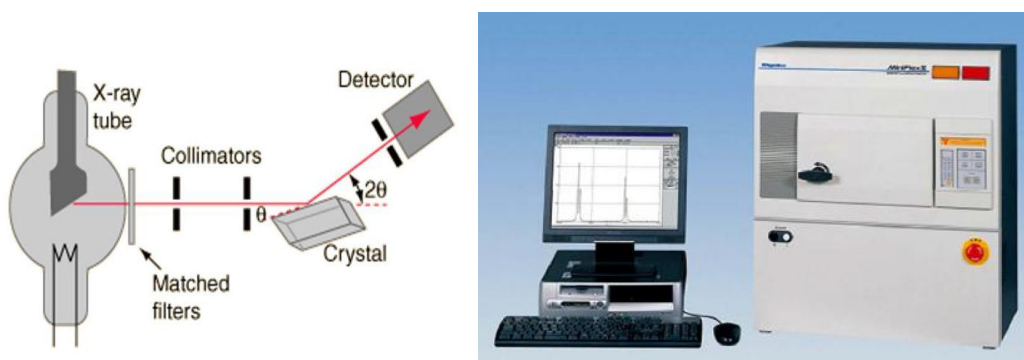


**Figure. 2.2:** The left figure depicts the schematic diagram of a XRD machine. The right figure is showing the X-ray diffractometer Rigaku Miniflex-II which we have used.

### 2.1.2.2 Neutron diffraction:

The powder neutron diffraction is one of the most powerful techniques available to the solid state physics research field for determining the crystal structure as well as the magnetic micro-spin structure. Neutrons are neutral and deeply penetrating unlike other radiation

sources e.g. x-ray and electrons. As a matter of fact, the wavelength of the incident neutrons having the same order of magnitude as the inter-atomic distances of crystalline solids enables one to study the aspects of condensed matter at atomic level.

### 2.1.2.2.1 Basic working principle

Eventually, all the diffraction experiments rely on the Bragg's law and there are mainly two ways of carrying out the experiment. In the first process, a monochromatic neutrons beam of wavelength  $\lambda_0$  is targeted on a sample and thus different inter-planar d-spacings are measured by moving a detector in a wide range of angles such that  $\lambda_0 = 2d_{hkl} \sin \Theta_{hkl}$ , where the Miller indices (hkl) are related to the inter-planar spacing  $d_{hkl}$ . The kinds of experimental techniques based on this method are called constant wavelength or steady state diffractometers. This method is usually used in most of the neutron diffraction facilities. However, there is an alternative method where the detector is kept fixed at an angle  $\Theta_0$  and the wavelength is varied. This can be done by utilizing a white spectrum having a broad range of wavelength and an energy dispersive detector. In this case, the d -spacings are found using the following relation:  $\lambda = 2d \sin \theta_0$ .

The neutrons interact with matter in two main ways: firstly, the strong nuclear interaction which is related to the interaction occurring between the neutron and the nuclei of the sample, thus producing the nuclear scattering; secondly, the magnetic interaction, which is related to the interaction occurring between neutron spin and the atomic spins of the sample under investigation, thus giving rise to the magnetic scattering. Hence, the neutron diffraction technique has numerous advantages over the X-ray diffraction technique. First, the scattering length which characterizes the nuclear interaction is not dependent on the atomic number  $Z$ , unlike the X-rays scattering length which is proportional to  $Z$ . This is the reason why for X-rays, the atoms having lighter weight are almost invisible (especially in the case when other heavy atoms are present), on the contrary, for the neutrons, both the light and

heavy atoms may have comparable scattering lengths. Secondly, as the neutrons have the magnetic spin moments, it interacts with the atomic spins of the sample and is capable of giving precise information about the spin structure of a system. Hence, the neutron diffraction technique is ubiquitous in the field of magnetism research.

The properties of neutrons are summarized below:

$$\text{Mass} = 1.674 \times 10^{-27} \text{ Kg}$$

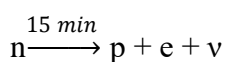
$$\text{Wavelength } \lambda = h/mv = h / (2mE)^{1/2} = 0.0286/E^{1/2}$$

$$\text{Charge} = 0$$

$$\text{Spin (s)} = \frac{1}{2}$$

$$\text{Magnetic dipole moment } \mu_N = -1.913$$

$$\text{Neutron life time: } 881.5 \pm 1.5 \text{ s } (\sim 15 \text{ min})$$



Neutron production is done in the reactor as follows:

### Reactor source



The fission neutrons have high KE 1-15 MeV

All of our neutron diffraction measurements were carried out on the PD2(Powder Diffractometer-2)neutron powder diffractometer ( $\lambda = 1.2443 \text{ \AA}$ ) at the Dhruva reactor in Bhaba Atomic Research Centre, Mumbai, India. The schematic diagram of neutron diffractometer set up PD-2 is given below:

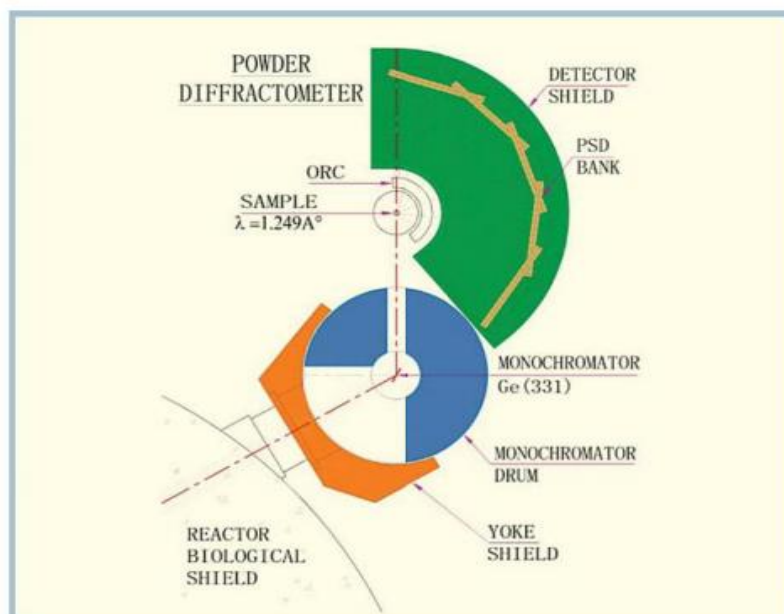


**Figure.2.3** :Setup PD-2 (Powder Diffractometer-2) at Bhabha Atomic Research Center, Mumbai, India.

### 2.1.2.3 Magnetic Property Measurement System (MPMS): SQUID-VSM

A superconducting quantum interference device (SQUID) is a device which is used to measure very small magnetic field changes with very high precision. The working principle of SQUID is based on the theoretical works by Josephson and was experimentally realised in 1963 for the first time. There are two different types of SQUIDs which are made up of a superconducting ring interrupted at a point (radio frequency-SQUID) or two points (dc-SQUID) using a normally conducting or electrically insulating material. However, this interruption must be thin enough so that the superconducting Cooper pairs can tunnel through this layer (Josephson contact). The basic function of a SQUID is based on the Josephson effect and the flux quantization effect in superconducting rings. Eventually, through a

superconducting ring only flows a magnetic flux whose size is an integral multiple of the elementary magnetic flux quantum  $\Phi_0 = 2.07 \times 10^{-15}$  Tesla-m<sup>2</sup>.

### 2.1.2.3.1 Principles

*A radio frequency (RF) SQUID:* It comprises of one Josephson junction, which is mounted on a superconducting ring. An oscillating current is supplied to an external circuit, whose voltage changes as an effect of its interactions with the ring. The magnetic flux is then measured.

*The DC SQUID:* A DC SQUID is basically a simpler device which is made up of two Josephson junctions connected in parallel on a closed superconducting loop as shown in Fig. 2.4(a) [1]. As already stated, a fundamental property of superconducting rings is that they can enclose flux quantum,  $\Phi_0 = 2.07 \times 10^{-15}$  Tesla-m<sup>2</sup>. In fact, the flux quantum is very small due to which this physical effect can be exploited to produce an extraordinarily sensitive magnetic detector known as the SQUID. The SQUIDs act as magnetic flux-to-voltage transducers where the sensitivity is set by the magnetic flux quantum. On application of the current to the SQUID (biasing it), it causes the Cooper pairs of electrons to tunnel through the junctions. However, the application of a magnetic field to the ring changes the flow. Actually, it alters the quantum-mechanical phase difference across each of the two junctions. The critical current of the SQUID is thus affected by these phase changes. As a consequence, a progressive rise or reduction in the magnetic field gives rise to the oscillations of the critical current between a maximum value and a minimum one. The maximum occurs when the flux administered to the SQUID equals an integral number of flux quanta through the ring; the minimum value corresponds to a half-integral number of quanta. The flux applied to the SQUID can assume any value, unlike the flux contained within a closed superconducting ring, which must be an integral number. In practice, the current is not measured instead the voltage across the SQUID swinging back and forth under a steadily changing magnetic field is measured (Fig. 2.4(b)). A digital magnetometer is based on this SQUID where, each "digit" corresponds to one flux quantum. As a matter of fact, the conventional electronics can even detect voltages corresponding to changes in magnetic flux of much less than one flux quantum. Hence, the SQUID can be realized as a flux-to-voltage transducer, transforming an extremely small change of magnetic flux into a voltage.

We have used the "Quantum Design MPMS 3" magnetometer throughout our research work for magnetic measurements. This MPMS set-up consists of three possible



measurement modes, DC scan mode, AC susceptibility mode, and vibrating sample magnetometer (VSM) mode. In contrast to the dc magnetization measurements, the ac susceptibility measurement is a unique tool for probing the spin dynamics. The VSM is based on Faraday's law of induction which states that an alternating magnetic field will induce an electric field and vice-versa. In VSM operation, a sample (powder/pellet) is kept within a uniform magnetic field and consequently, they get magnetized by aligning the magnetic domains in the direction of the field. However, the magnetization of the sample will in turn induce a magnetic field near the sample, known as a stray magnetic field of the sample. When the sample vibrates, this stray magnetic field alters as a function of time. This change is sensed by a set of pick-up coils. The pick-up coil is SQUID based and thus has a very high sensitivity. This induced current is directly proportional to the magnetization of the sample. The induction current is then amplified by a trans-impedance amplifier and a lock-in amplifier. The various components are connected to computer resources. Controlling and monitoring software is used to perform several experiments following different protocols.

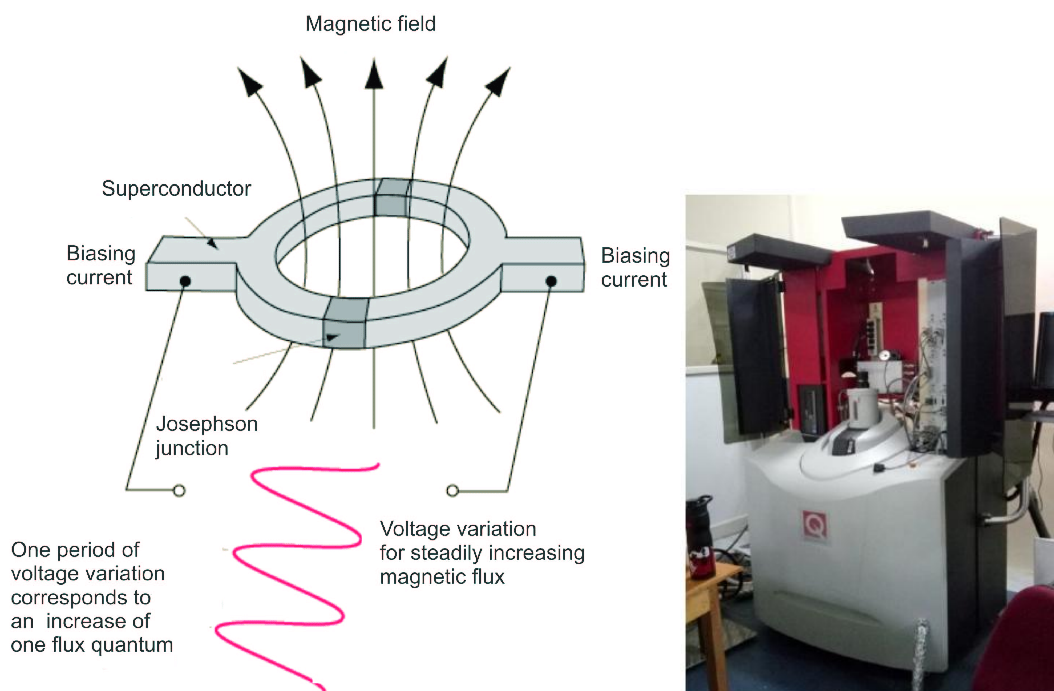


**Figure.2.4** : (a) depicts the Josephson junction. (b) shows the picture of the Quantum Design MPMS SQUID VSM facility in our institute.

### 2.1.2.4 X-ray Photoemission Spectroscopy(XPS)

The X-ray Photoemission Spectroscopy (XPS) which is also called as photoelectron spectroscopy for Chemical Analysis (ESCA), is a powerful technique used to collect chemical information about the surfaces of solid materials viz., oxidation states, elemental composition, ligand co-ordination etc [2]. Both the insulators and conductors can easily be investigated in surface areas from a few microns to a few millimetres depth. In fact, the XPS is a surface sensitive technique since it mainly detects those electrons generated near the surface. The photoelectrons of interest have comparatively low kinetic energy. As a consequence of the inelastic collisions in the sample's atomic structure, photoelectrons producing more than 20 to 50 Å beneath the surface cannot escape with sufficient energy to be detected in this technique.

#### 2.1.2.4.1 Working principle:

The sample under investigation is kept inside an ultrahigh vacuum ambience (typically  $\sim 10^{-10}$  torr) and then it is exposed to a monochromatic, low-energy X-ray source. The X-rays incident on the sample results in the ejection of core-level electrons from sample atoms. In fact,

the energy of a core electron produced in such photoemission process is a function of its binding energy and is a characteristic of the element from which it was emitted. As a matter of fact, the primary data used for XPS is the energy analysis of the photo-emitted electrons. When the incident X-ray ejects the core electron, an outer electron fills the core hole. The energy of this transition is balanced by the emission of an Auger electron or a characteristic X-ray. Analysis of Auger electrons can also be utilized in XPS, in addition to emitted photoelectrons.

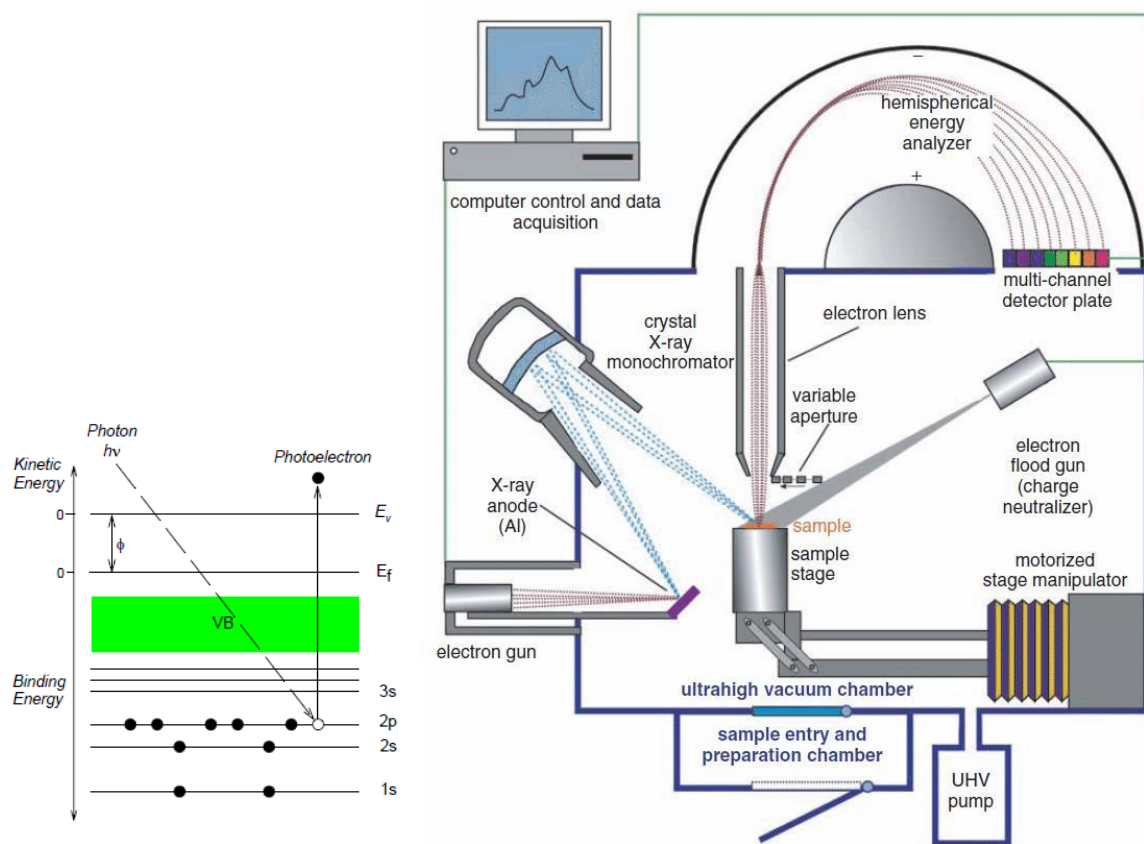


**Figure. 2.5:** The left figure shows the schematic diagram of photoelectric effect. The right figure depicts the schematic diagram of a XPS set-up.

The energy of each of the photoelectrons can be estimated by using an equation based on the work of Ernest-Rutherford (1914):

$$E_{\text{kinetic energy}} = h\nu - (E_B + \phi)$$

where  $E_B$  is the binding energy (BE) of the electron,  $h\nu$  is the energy of the X-ray photons being used,  $E_{\text{Kinetic energy}}$  is the kinetic energy of the electron that measured by the instrument and  $\phi$  is

the work function of the spectrometer (not the material). This is shown in the schematic diagram Fig. 2.5 (left).

*The different instrumental units of a XPS machine (shown in the schematic diagram in Fig. 2.5-right)*

1. Hemispherical electron energy analyzer
2. X-ray source.
3. Ar-ion gun.
4. Vacuum system.
5. Neutralizer or electron flood gun.
6. Multi-channel detector plates.
7. Sample stage or holder.
8. Electronic control units.
9. Computer.

### **2.1.2.5 Raman Spectroscopy**

In the year 1928, Raman and Krishnan had discovered the Raman spectroscopy [3]. However, during his discovery, very crude instrumentation was available such as he used sunlight as the source, a telescope as a collector and he used his eyes as detector! Thereafter, lots of improvements were furnished. At first, innovation of a good excitation source was looked for. Then, the detector system was invented and a commercial Raman spectrometer was available. Since then, it remained as a novel qualitative and quantitative spectroscopic technique for probing the dynamic crystal structure by the scattering of radiation.

#### **2.1.2.5.1 Basic principle:**

During the scattering of the light from a molecule or crystal, most photons are elastically scattered. Hence, such scattered photons have exactly the same energy and, therefore,

wavelength, as the incident light. As a matter of fact, only a small fraction of light (approximately 1 in  $10^7$  photons) suffers inelastic scattering, leading to a change in its frequency. The mechanism leading to the inelastic scattering is known as the Raman Effect. In fact, the Raman scattering can occur giving rise to a change in vibrational, rotational or electronic energy of a molecule. The case of the elastic scattering is known as the Rayleigh scattering.

The Raman effect is based on molecular deformation in electric field  $E$  determined by molecular polarizability  $\alpha$ . The laser beam can be considered as an oscillating electromagnetic wave with electric vector  $E$ . After interaction with sample it induces electric dipole moment  $P = \alpha E$  which deforms molecule. Due to the periodical deformation, molecules start vibrating with characteristic frequency  $\nu_m$ . Amplitude of vibration is defined as nuclear displacement or it can be realized by another way: monochromatic laser light  $\nu_0$  excites molecules and transforms them into oscillating dipoles. That oscillating dipoles emit light of three different frequencies such as  $\nu_0$ ,  $\nu_0 - \nu_m$  and  $\nu_0 + \nu_m$  which are known as Rayleigh, Stokes and Anti-Stokes scattering (as shown in Fig. 2.6).

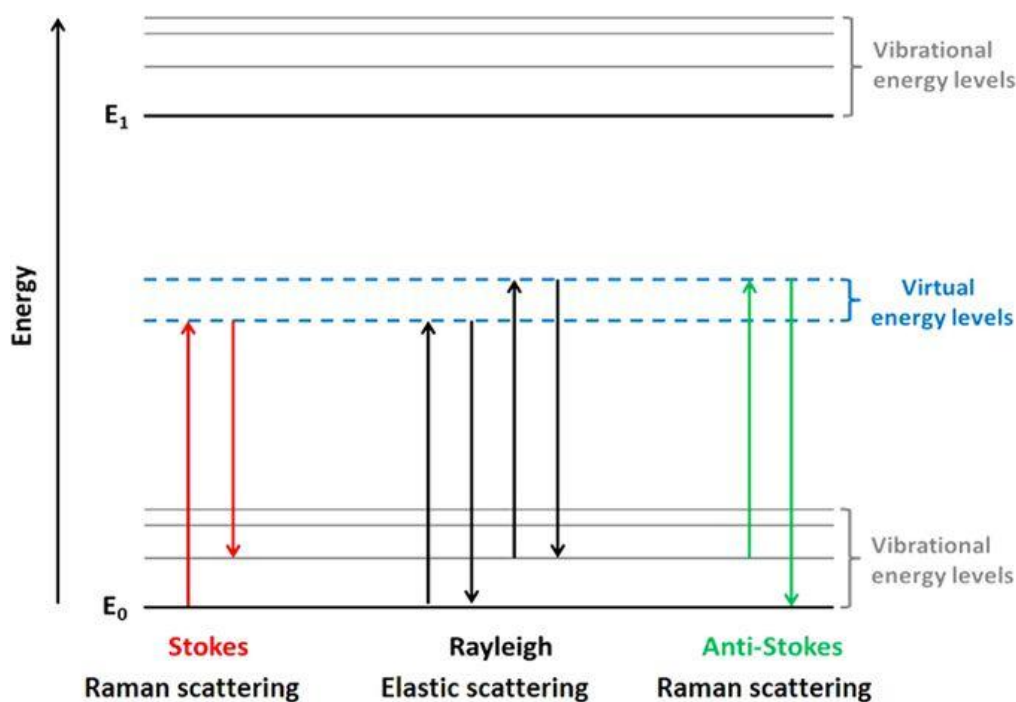


**Figure.2.6 :** Energy level diagram showing states involved in Raman effect.

### 2.1.2.5.2 Brief description of the Raman spectrometer used:

In Raman spectroscopy, laser light of particular wavelength is targeted on the sample which interacts with molecular vibrations or other excitations of the system. As a consequence of this interaction, change occurs in energy of the laser photons either by increasing it (shifted up) or decreasing it (shifted down) as already discussed. This shift in energy (Raman shift) of the scattered light carries information about the vibrational and/or rotational modes remaining in the system. The Reinshaw Raman spectrometer is equipped with a 532 nm laser (Fig. 2.7). An additional attachment of liquid nitrogen set-up allows one to perform the temperature dependent Raman spectroscopy by this. The pump source is a diode-pumped solid-state laser (DPSSLs) of wavelength 532 nm having a maximum power of 100 mW, 5% of which have been used to avoid laser-induced heating in the materials. The incident laser beam comes to a focus at a very short working distance over a 50× long-distance objective linked to the Leica DM 2500M microscope. As a dispersion element 2400 groves/mm grating is installed and to maintain the constant phase, the slit width of 50 micron is kept fixed throughout the experiments. The radiation after scattering is collected at back scattered position which is passed through the filter to eliminate the unwanted part of radiation. Thereafter, the radiation is fed to the detector. The resolution of the spectrometer is more than  $1 \text{ cm}^{-1}$  with deviation from the ideal spectrum less than  $\pm 0.2 \text{ cm}^{-1}$ . Using the supplied 4.0 software Spectrometer scanning, data collection, and processing were done.



**Figure.2.7:** *Renishaw micro Raman spectroscope.*

### 2.1.2.6 X-ray absorption spectroscopy

In X-ray spectroscopy studies, the involved transitions are related to the either absorption (X-ray absorption spectroscopy) or emission (X-ray photoemission spectroscopy) of X-rays, in which the former measures the ground state to the excited state transitions, while the later investigates the decay process from the excited state. However, both the techniques can probe the chemical states and local environment of atoms in molecules. In X-ray absorption spectroscopy (XAS), the incident X-ray photon excites an electron in the core level to an unoccupied conduction level following the intra-atomic dipole selection rule. Since the energy difference of the core level and conduction level are specific to the elements, XAS is an element specific probe. The synchrotron based XAS is a spectroscopic tool to probe electronic states of a matter. The synchrotron based XAS facilities provide a wide range of X-ray energies that are capable of sensing the most of the elements in the periodic table. In contrast to the other methods (such as optical or UV absorption, magnetic susceptibility, fluorescence, electrochemistry etc.), the XAS technique uses a previously chosen energy of

the incident X-rays to identify the specific element being probed. For last few decades it is being widely used due to its element specificity, sensitivity to the spin orientation and the surface sensitivity. Like X-ray photoemission spectroscopy (XPS), XAS is used for quantitative analysis of the oxidation states of the elements of a material. However, additionally, XAS has an intrinsic capability to sense magnetic ordering also. The circular polarization of the synchrotron X-ray makes it possible to investigate the spin orientation of the magnetic materials. This information of magnetic ordering is embedded in the same multiplet structure which is used to specify the presence of different chemical species. The signature of ferromagnetic or antiferromagnetic etc. ordering is seen as an increase or decrease of some peak intensities in a particular multiplet pattern. Therefore, it is necessary to have knowledge of both the shape of the spectra signifying a specific element as well as the possible alterations in those spectra which accompany different type of magnetic orderings. Thus, if we have this information beforehand, the magnetic information can be extracted not only for a specific element but also for different chemical phases of that same element.

The X-ray absorption spectra of any system such as atomic or molecular in nature are characterized by sharp rises in absorption at specific X-ray photon energies that are characteristic feature of the absorbing element. These sudden rises in absorption are known as absorption edges. It is related to the energy necessary to eject a core electron into the LUMO or to the continuum thus producing a photoelectron. The absorption discontinuity rising due to the photoelectron originated from a 1s core level is known as K-edge. It is called L-edge when the ionization is from a 2s or 2p electron. Similarly, it is called the M-edge when the photoelectrons excites from a 3d electrons.

All of our XAS measurements were performed at the BL14 beamline of Hiroshima Synchrotron Radiation Centre, Hiroshima University, Japan. In recording the spectra, total



electron yield (TEY) mode has been used as it requires relatively easy experimental setup and gives high signal to noise ratio. A base pressure of  $4 \times 10^{-8}$  Pa was maintained in the experimental chamber where the sample was mounted. The photon energy range of the beamline was 400-1200 eV which is compatible for XAS study at *K, L and M* edges of different elements.

### 2.1.2.7 Resistivity measurements

The temperature dependent resistivity measurements were performed using helium based closed cycle refrigerator (CCR) along with Keithley 2400 source meter or Keithley 6517B electrometer (used for measuring relatively high resistivity) and a Cryocon 32B temperature controller. The pellets of 10 mm diameter with small thickness (1-2 mm) are used for the measurements. The two faces of such pellets are coated with conducting silver paste and two copper wires are attached with it. After the sample is mounted in the CCR chamber, a high vacuum with turbo molecular pump is created inside the chamber. Thereafter, the temperature variation of the resistivity is measured.

### References

1. J. Clarke, *Scientific American* 271, 46 (1994)
2. C. Fadley, *J. Electron spectroscopy and Related Phenomena* 178, 2 (2010)
3. C. V. Raman and K. S. Krishnan, *Nature* 121, 501 (1928)

